Characterisation of hybrid metal matrix syntactic foams

Imre Norbert ORBULOV [1,2,a], Kornél MÁJLINGER[1,b]

[1]Budapest University of Technology and Economics Faculty of Mechanical Engineering
Department of Materials Science and Engineering, Bertalan Lajos u. 7., 1111 Budapest, Hungary

[2]MTA-BME Research Group for Composite Science and Technology, Műegyetem rkp. 3-11., H-1111 Budapest, Hungary

[a]orbulov@eik.bme.hu (corresponding author), [b]vmkornel@eik.bme.hu

Abstract. High quality aluminium matrix syntactic foams (AMSFs) were produced by pressure infiltration. This method can ensure the maximal volume fraction of the reinforcing hollow spheres and very low amount of unwanted or matrix porosities. By this method hybrid MMSFs with mixed metal and ceramic hollow spheres were also produced. The matrix material was AlSi12 alloy and two different types – produced by Hollomet GmbH in Germany – of hollow spheres were used: Globomet (GM) and Globocer (GC). The geometrical properties of the hollow spheres were similar (average outer diameter), but their base material was pure iron and $Al_2O_3+SiO_2$ in the case of GM and GC hollow spheres respectively. The volume fraction of the reinforcing hollow spheres were maintained at ~65 vol%, but the ratio of them was altered in 20% steps (100% GM + 0% GC, 80% GM + 20% GC…). The results of the compression tests showed, that the compressive strength, yield strength, plateau strength, structural stiffness and the absorbed mechanical energy values increased with higher ceramic hollow sphere reinforcement ratio. The fracture strains of the investigated MMSFs decreased with the higher GC ratio. Generally the strength values also increased with higher diameter to height (H/D) ratio from H/D=1 to H/D=1.5 and 2.

Introduction

Metal matrix syntactic foams (MMSFs) are special composites that consists different size and material hollow spheres as reinforcement. Due to the hollow structure and beneficial strength of the spheres these composites behave like strong metallic foams, with at least two times higher compressive strength and energy absorbing capacity, than conventional ones. In MMSFs, the matrix material is usually some kind of aluminium alloy, but Fe matrix variants [1, 2] and Mg [3, 4], or Zn [5, 6] based versions are also known.

Nowadays MMSFs are investigated more and more intensively. Most of the published papers focus on the production and/or mechanical properties of the foams [7, 8]. Some of the works gives overall review on the investigated MMSF systems that are most important, for example Santa-Maria et al. and Fergusson et al. investigated the microstructure and quasi-static compressive mechanical properties of Al-A206/Al_2O_3 MMSFs. They found that the peak strength, plateau strength and toughness of the foams were increased with increasing wall thickness to diameter ratio [9-10]. The expected mechanical properties were also predicted by mathematical model [10]. The mechanical response of the MMSFs is also important in the case of high strain rate loading too. In the case of collision damping or other, energy absorbing applications high loading speeds can occur. Luong et al. [11-13] investigated the MMSFs in this point of view and found that while the matrix alloy does

not show any appreciable strain rate sensitivity, the composite shows higher strength at higher strain rates. The energy absorption capability of MMSFs is found to be higher at higher strain rates.

In the published papers, the MMSFs usually have a simple reinforcement that means only one grade of well-defined hollow spheres are applied. However there is a possibility to use for example bimodal reinforcement [14] or different grade reinforcement to produce hybrid MMSFs. Due to this our main goal was to produce such hybrid MMSFs and report their properties.

Materials and methods

Constituents and production method

As matrix material near eutectic AlSi12 alloy (Al4047) was used due to its low melting point (~575°C) and low viscosity. Besides Al the material contained 12.83 wt% Si and about 0.2 wt% other elements (Fe, Cu, Mn, Mg, Zn). This composition is in the range of the nominal values. The reinforcement consists of two different types of hollow spheres (one ceramic and one metal) manufactured by Hollomet GmbH. The ceramic hollow spheres (Globocer, GC) had the average diameter of Ø1450 μm and average wall thickness of t=60 μm. Their density was ρ=0.816 gcm^{-3}. The hollow sphere's wall material was built up from ~30 wt% Al_2O_3, ~50 wt% SiO_2 and ~20 wt% $3Al_2O_3 \cdot 2SiO_2$. The metallic hollow spheres (Globomet, GM) had the similar average diameter and wall thickness, while their density was ρ= 0.4 gcm^{-3}. The ratio of the hollow spheres was varied from 100% GM and 0% GC to 0% GM and 100% GC, in 20% steps. The hybrid ASFs were produced pressure infiltration technique (Fig. 1). The mechanically mixed hollow spheres were put into a ~360 mm height, graphite coated carbon steel mould (cross section: ~40×60 mm) to the half and they were densified by gentle tapping to get ~65 vol% volume fraction, that corresponds to randomly closed packed structure. Subsequently, a layer of alumina mat was placed on the hollow spheres and a block of matrix material was inserted on the mat. The mould was put into the infiltration chamber; the furnace was closed and evacuated by a vacuum pump to a rough vacuum.
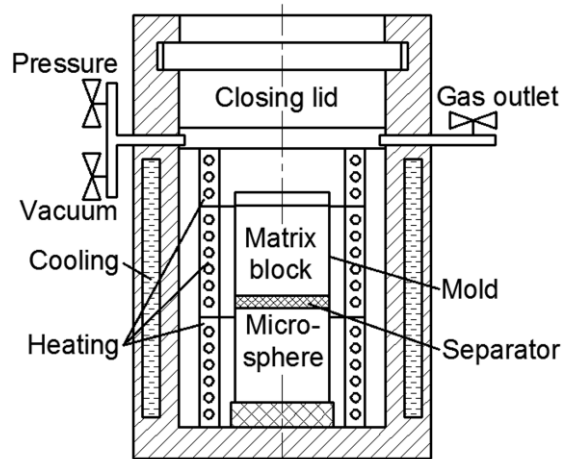
Figure 1. Schematic sketch of the infiltration setup

Table 1. Measured density values of the AMSFs

Reinforcement	Measured density, ρ_m (gcm^{-3})
100GM-0GC	1.327
80GM-20GC	1.639
60GM-40GC	1.649
40GM-60GC	1.694
20GM-80GC	1.743
0GM-100GC	1.833

During the heating the temperatures of the matrix block and the hollow spheres were monitored by two thermocouples. After melting of the matrix material the fluid sealed the mould above the separator layer. Subsequently, Ar gas was let into the chamber at 400 kPa to perform the infiltration. After slow cooling and solidification the mould was removed from the chamber and further cooled to room temperature in water. Then the AMSF block (~40×60×180 mm) was removed from the mould. The blocks were designated after their constituents, for example 80GM-20GC stands for an AMSF block with ~65 vol.% of hollow spheres that is mixed from 80% GM and 20% GC hollow spheres respectively. The measured composite densities (ρ_m) are listed in Table 1.

Experimental

Scanning electron microscopy (SEM) investigations and line EDS (energy dispersive spectroscopy) were done on a Phillips XL-30 type electron microscope and its EDAX Genesis EDS attachment on
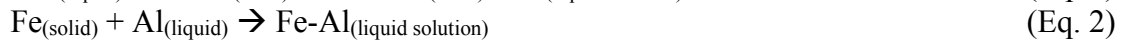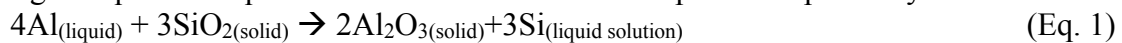
polished surfaces. The measurements started from the matrix and crossed the wall of the hollow sphere. Along each line thirty points were evaluated. The points were excited for 15 s with 35 µs amplification time.

The compressive properties were determined in quasi-static conditions on Ø14 mm cylindrical specimens. The aspect ratio (H/D) of the specimens was varied and was set to1, 1.5 or 2. The compression tests were done on a MTS 810 type hydraulic testing machine in a four column tool at room temperature. The surfaces of the tool were polished and lubricated. The speed of the test was set to 0.01 s^{-1}. From each specimen group five specimens were compressed up to 25% engineering strain (in summary 90 tests were done). The recorded curves were evaluated in accordance with the ruling standard DIN50134. The investigated properties were: compressive and flow strength, fracture strain, structural stiffness and absorbed energies.

Results and discussion

Microstructural investigations
The quality of infiltration was investigated by optical microscopy and SEM. The observations showed almost perfect infiltration, the cavities between the hollow spheres were fulfilled by the AlSi12 matrix. The uninfiltrated void content between the hollow spheres remained minimal, below 3%. Some hollow spheres were broken and therefore infiltrated. Most of the infiltrated spheres were GM grade, because the molten AlSi12 can dissolve pure Fe from the wall it was weakened and lead to the infiltration of the hollow spheres. The molten matrix can react with the reinforcement according to Eq. 1 and Eq. 2-4 in the case of GC and GM spheres respectively.

$$4Al_{(liquid)} + 3SiO_{2(solid)} \rightarrow 2Al_2O_{3(solid)} + 3Si_{(liquid\ solution)} \qquad \text{(Eq. 1)}$$
$$Fe_{(solid)} + Al_{(liquid)} \rightarrow Fe\text{-}Al_{(liquid\ solution)} \qquad \text{(Eq. 2)}$$
$$Fe_{(solid)} + 3Al_{(liquid)} \rightarrow Al_3Fe_{(solid)} \qquad \text{(Eq. 3)}$$
$$Fe_{(solid)} + Si_{(liquid\ solution)} \rightarrow FeSi_{(solid)} \qquad \text{(Eq. 4)}$$

The diffusion reaction described in Eq. 1 was induced by the Si concentration mismatch between the material of the hollow spheres and the matrix. However, this exchange reaction was constrained by the high Si amount in the matrix. The properties of the interface layer between matrix and reinforcements were investigated by EDS along distinguished lines perpendicular to the wall of the spheres. A typical site of 40GM-60GC AMSF is shown in Fig. 2. The SEM micrograph of a GM (left) and GC (right) hollow spheres near to each other and the path of the line EDS analysis (arrow) are shown in Fig. 2a, and the chemical composition along the investigated line in Fig. 2b. The SEM image shows unharmed hollow spheres and the less than 100 µm gap between the GM and GC hollow spheres and the matrix prove the good infiltration.
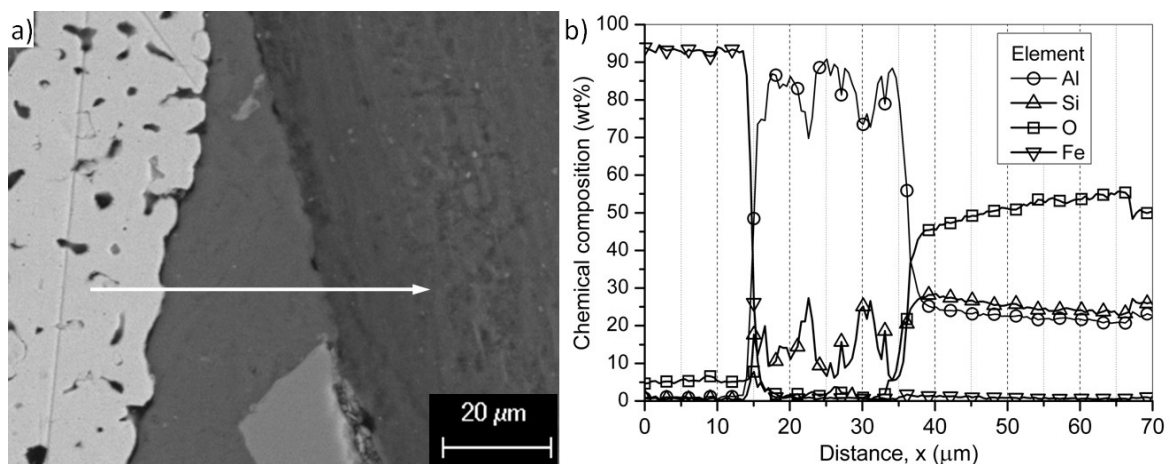
Figure 2. a) SEM image of 40GM-60GC sample of a GM (left) and GC (right) hollow spheres and the line of the EDS analysis (arrow), b) the chemical composition along the investigated line

The chemical composition along the analysis line follows the actual composition of the wall, the interface and the matrix respectively. The first couple of micrometers measured in the GM hollow

sphere showed Fe and some O due to the oxidization of the specimen's surface. Between the spheres Si peaks can be detected beside the dominant Al, because of the eutectic matrix material. In the GC hollow spheres the Al-Si-O ratio followed the composition of the ceramic wall. Because of the interface layers between the hollow spheres and the matrix material sudden changes can be observed in the chemical composition. These narrow zones indicate thin interface layers. The thickness of these layers can be estimated from the slope changes of the differentiated Fe and O curves and it was between 5 μm and 7 μm in the case of GM and GC hollow spheres respectively.
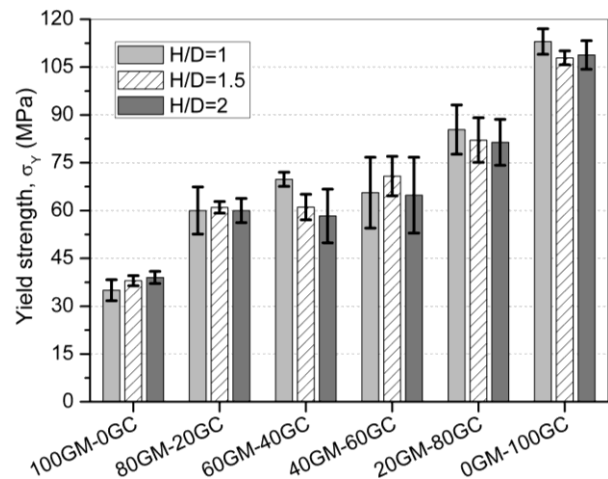
Compressive properties

The compression tests were evaluated according to the standard (DIN50134) about the compression tests of cellular materials. The strength of MMSFs was characterised by (i) the first stress peak (compressive strength, σ_c), (ii) the strength at a given plastic deformation (similar to yield strength, σ_y) and (iii) the plateau strength (σ_p, the average stress level in the second half of the compressive curve). The deformation capability can be described by is the fracture strain (ε_c), that is the strain at σ_c. The elastic behaviour of the AMSFs can be characterised by the slope of the initial part of the stress – strain curve, called structural stiffness (S). The fracture energy (the absorbed energy up to the fracture strain, W_c), and the area under the stress-strain curve as the whole absorbed energy (W) were further monitored properties. The energies can be determined by the numerical integration of the stress-strain curves up to the fracture strain or up to 25% in the case of fracture energy and the overall absorbed energy respectively.

Fig. 3 plots the measured compressive strength values as the function of aspect ratio and the ratio of the hollow sphere types. (In the case of pure GM reinforcement, pronounced compressive strength could not be determined; therefore the yield strength was plotted for comparison). There are some notable trends in the measured values: the smaller specimens were stronger and the compressive strength also increased with the amount of the GC grade reinforcement. The gradient of this increment was rather moderate: as the amount of the weaker, plastically deformable GM fraction decreased, the compressive strength increased proportionally. In the case of pure GC reinforcement a higher increment was observed: the stronger GC spheres and the lack of plastically deformable GM hollow spheres ensured higher strength niveaus and altered the fracture mechanism. Identical behaviour can be concluded from the yield strength values (Fig. 4).
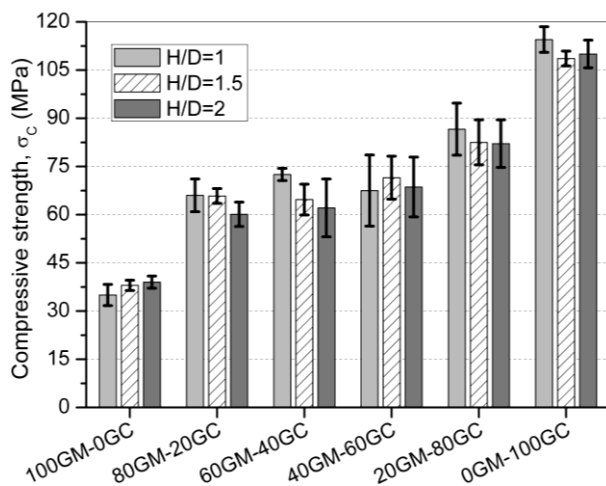
Figure 3. Compressive strength values   **Figure 4.** Yield strength values

The AMSFs with GM type reinforcement had no pronounced compressive strength, but a long and almost constant plateau region with completely plastic deformation (like 'conventional' metallic foam). Due to the unique built up and deformation of each sample the scatter of the plateau were somewhat larger (Fig. 5). By the gradual increment of the GC fraction, the compressive strength became more pronounced and the failure mechanism also turned to brittle mode with a sharp, severely compressed fracture band. The trends of the fracture strain values (Fig. 6.) confirmed the above detailed effect. As the volume fraction of the ceramic GC hollow spheres increased, the fracture strain decreased significantly and the failure mode became brittle. The aspect ratio had

similar effect on the fracture strain: the higher aspect ratio resulted in intensified shearing and due to this; the fracture occurred earlier. This effect was more emphasized in the case of higher GC content, because the sensitivity to shearing of the ceramic materials. The structural stiffness values changed at the contrary (Fig. 7.). The highest stiffness was measured in the case of H/D=2 in the case of the highest GC content. The aspect ratio had linear connection with the structural stiffness, but the increment of the GC hollow sphere fraction had an exponential effect on the stiffness.
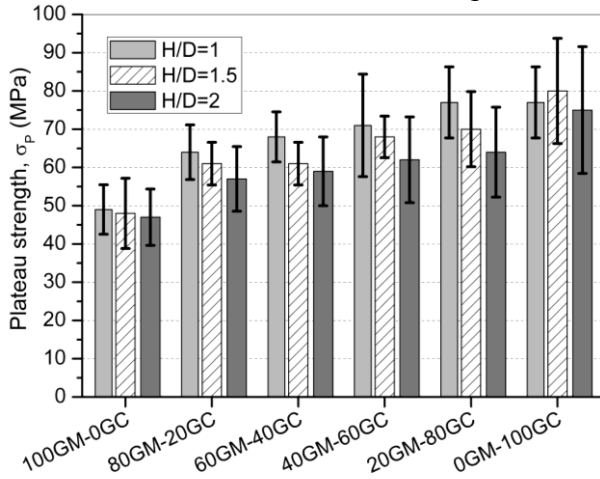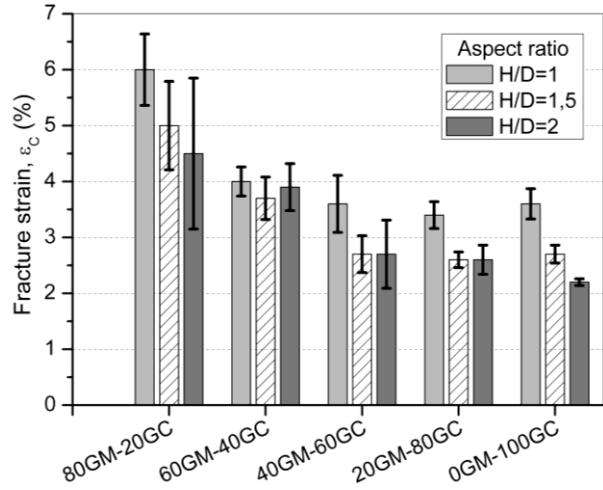

Figure 5. Plateau strength values

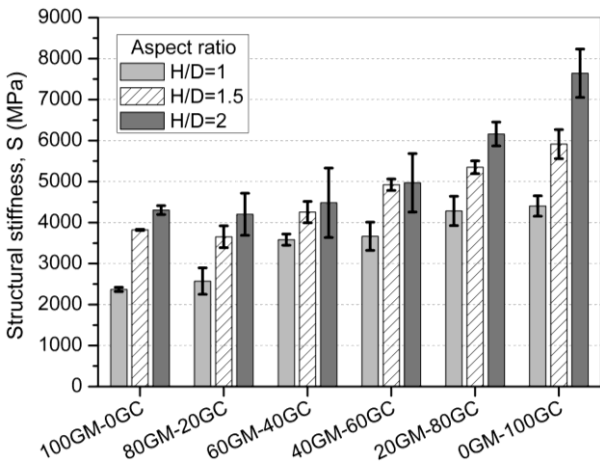**Figure 6.** Fracture strain values

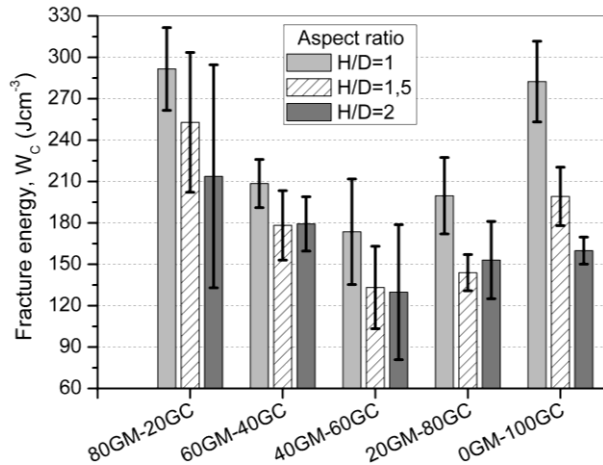

Figure 7. Structural stiffness values

Figure 8. Fracture energy values

The fracture energy (Fig. 8) had a maximum in the case of pure GC reinforcement: the strong ceramic hollow spheres ensured high compressive and plateau stress levels; therefore the absorbed energy was high. As the weaker GM grade spheres were built in, the compressive strength and the fracture energy decreased. In the case of higher GM hollow sphere fraction (>40%) the fracture energy increased again: the decrement of the compressive strength was balanced by the plastic deformation capability, i. e. the higher fracture strain of the AMSFs (wider limits for the integration) and despite the lower compressive strength the fracture energy could become higher. Similar behaviour can be observed in the overall absorbed energy
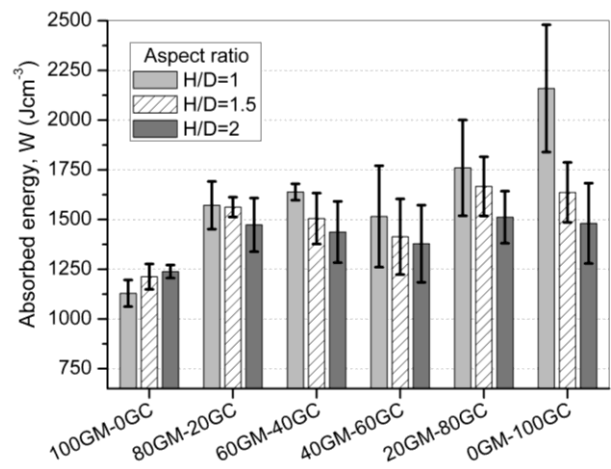

Figure 9. Overall absorbed mechanical energy values

(calculated up to 25%, Fig. 9). The expected high energy absorption capacity could not be observed in the case of pure GM grade reinforcement due to their very low compressive and plateau strength.

Summary

From our investigations and results, the following statements can be concluded:

- Pressure infiltration is a reliable hybrid ASF production method. The process can ensure high hollow sphere content and low uninfiltrated porosity.
- The line EDS measurements indicated (i) solution of Fe from GM hollow spheres and (ii) an exchange reaction between the AlSi12 matrix and the GC hollow spheres into the AlSi12 matrix. Both process can cause damage to the wall and leads to infiltrated hollow spheres.
- The ratio of the GC and GM grade hollow spheres had strong influence on the mechanical properties of the produced AMSFs. The strengths and the stiffness increased by the increment of GC content.
- Both the fracture energy and the overall absorbed energy values had a local minimum in the case of 60GC+40GM reinforcement. Higher GC content resulted in higher compressive and plateau strengths and due to this the absorbed energies became higher. Lower GC content resulted in lower the strength values, but the ductility of iron GM hollow spheres could balance and overcome this effect.

Acknowledgements

References

[1] L. Peroni, M .Scapin, M. Avalle, J. Weise, D. Lehmhus, Dynamic mechanical behavior of syntactic iron foams with glass microspheres, Mater Sci Eng A. 552(0) (2012) 364-375.

[2] L. Peroni, M .Scapin, M. Avalle, J. Weise, D. Lehmhus, J. Baumeister, M. Busse, Syntactic Iron Foams - On Deformation Mechanisms and Strain-Rate Dependence of Compressive Properties, Adv Eng Mater. 14(10) (2012) 909-918.

[3] A. Daoud, MT. Abou El-khair, M. Abdel-Aziz, P. Rohatgi, Fabrication, microstructure and compressive behavior of ZC63 Mg–microballoon foam composites, Compos Sci Technol. 67(9) (2007) 1842-1853.

[4] PK. Rohatgi, A. Daoud, BF. Schultz, T. Puri, Microstructure and mechanical behavior of die casting AZ91D-Fly ash cenosphere composites, Composites Part A. 40(6–7) (2009) 883-896.

[5] A. Daoud, Synthesis and characterization of novel ZnAl22 syntactic foam composites via casting, Mater Sci Eng A. 488(1–2) (2008) 281-295.

[6] A. Daoud, Effect of strain rate on compressive properties of novel Zn12Al based composite foams containing hybrid pores, Mater Sci Eng A. 525(1–2) (2009) 7-17.

[7] XF. Tao, YY. Zhao, Compressive failure of Al alloy matrix syntactic foams manufactured by melt infiltration, Mater Sci Eng A. 549 (2012) 228-232.

[8] PK. Rohatgi, N. Gupta, BF. Schultz, DD. Luong, The synthesis, compressive properties, and applications of metal matrix syntactic foams, JOM. 63(2) (2011) 36-42.

[9] JA. Santa Maria, BF. Schultz, JB. Ferguson, PK. Rohatgi, Al–Al2O3 syntactic foams – Part I: Effect of matrix strength and hollow sphere size on the quasi-static properties of Al-A206/Al2O3 syntactic foams, Mater Sci Eng A. 582 (2013) 415-422.

[10] JB. Ferguson, JA. Santa Maria, BF. Schultz, PK. Rohatgi, Al–Al2O3 syntactic foams—Part II: Predicting mechanical properties of metal matrix syntactic foams reinforced with ceramic spheres, Mater Sci Eng A. 582 (2013) 423-432.

[11] DD. Luong, OM. Strbik III, VH. Hammond, N. Gupta, K. Cho, Development of high performance lightweight aluminum alloy/SiC hollow sphere syntactic foams and compressive characterization at quasi-static and high strain rates, J Alloys Compounds. 550 (2013) 412-422.

[12] DD. Luong, N. Gupta, A. Daoud, PK. Rohatgi, High strain rate compressive characterization of aluminum alloy/fly ash cenosphere composites, JOM. 63(2) (2011) 53-56.

[13] DD. Luong, N. Gupta, PK. Rohatgi, The high strain rate compressive response of Mg-Al alloy/fly Ash cenosphere composites, JOM. 63(2) (2011) 48-52.

[14] XF. Tao, LP. Zhang, YY. Zhao, Al matrix syntactic foam fabricated with bimodal ceramic microspheres, Mater Des. 30(7) (2009) 2732-2736.